Perfusive and diffuse oxygen transport in skeletal muscle during incremental handgrip exercise

by

Shane Michael Hammer

B.S., Kansas State University, 2015

A THESIS

submitted in partial fulfillment of the requirements for the degree

MASTER OF SCIENCE

Department of Kinesiology
College of Human Ecology

KANSAS STATE UNIVERSITY
Manhattan, Kansas

2017

Approved by:

Major Professor
Dr. Thomas J. Barstow

Copyright

Abstract

Limb blood flow increases linearly with exercise intensity; however, invasive measurements of microvascular muscle blood flow during incremental exercise have demonstrated submaximal plateaus. Diffuse correlation spectroscopy (DCS) noninvasively quantifies relative changes in microvascular blood flow at rest via a blood flow index (BFI). The purpose of this study was to quantify relative changes in tissue blood flow during exercise using DCS, compare the BFI of the flexor digitorum superficialis (BFI_{FDS}) muscle to brachial artery blood flow ($\dot{Q}_{BA}$) measured via Doppler ultrasound, and employ near infrared spectroscopy (NIRS) alongside DCS to simultaneously measure perfusive and diffusive oxygen transport within a single volume of exercising skeletal muscle tissue. We hypothesized $\dot{Q}_{BA}$ would increase with increasing exercise intensity until task failure, BFI_{FDS} would plateau at a submaximal work rate, and muscle oxygenation characteristics (total-[heme], deoxy-[heme], and % saturation) measured with NIRS would demonstrate a plateau at a similar work rate as BFI_{FDS}. Sixteen subjects (23.3 ± 3.9 yrs; 170.8 ± 1.9 cm; 72.8 ± 3.4 kg) participated in this study. Peak power (P_{peak}) was determined for each subject (6.2 ± 1.4W) via an incremental handgrip exercise test to task failure. Measurements of $\dot{Q}_{BA}$, BFI_{FDS}, total-[heme], deoxy-[heme], and % saturation were made during each stage of the incremental exercise test. $\dot{Q}_{BA}$ increased with exercise intensity until the final work rate transition ($p < 0.05$). No increases in BFI_{FDS} or muscle oxygenation characteristics were observed at exercise intensities greater than 51.5 ± 22.9% of P_{peak} and were measured simultaneously in a single volume of exercising skeletal muscle tissue. Differences in muscle recruitment amongst muscles of the whole limb may explain the discrepancies observed in $\dot{Q}_{BA}$ and BFI_{FDS} responses during incremental exercise and should be further investigated.

Table of Contents

List of Figures

Acknowledgements

I owe much of my success to the phenomenal family, mentors, and friends that I have been so privileged to know.

Mom & Dad – You have instilled in me the value of hard work and dedication. I am so thankful for the many opportunities you have provided me. I love you.

Dr. Barstow – Your enthusiasm for science is contagious. I am tremendously grateful for your outstanding mentorship and guidance. You are an exceptionally great person and scientist.

Josh – Thank you for showing me what a great scientist, teacher, and colleague look like. You are an incredible role model. Most importantly, thank you for your friendship these past years.

Andrew & Kaylin – The relationships we have built with one another in such a short time are remarkable. I think of you both as a part of my family. Thank you for all of your hard work and exceptional collaboration. I am excited to see what the future holds.

Finally, I would like to thank all of my incredible friends (you know who you are). You have made this experience truly great. I love you all.

Dedication

This project is dedicated to my wife, Sarah, and to my daughter, Scarlett.

Sarah,

The sacrifices you have made to enable me to pursue my dreams are countless. I am forever grateful for your belief in me and endless support and encouragement.

I love you.

Scarlett,

I hope that one day you might read this and be proud of me. So much of what I do is for you.

I love you.

Chapter 1 - Introduction

A wealth of evidence exists demonstrating that bulk limb blood flow is tightly coupled to exercise intensity (2, 67). Measurements of bulk limb blood flow have been combined with blood gas measurements and estimates of fractional oxygen extraction to estimate muscle oxygen consumption during exercise using the Fick principle (2, 20, 36, 38). While informative, these measurements may not be indicative of tissue oxygen consumption and hemodynamic relationships at the level of gas exchange, i.e., tissue microvasculature.

Microvascular hemodynamics and muscle oxygen pressure dynamics following the onset of, and in recovery from, muscle contractions have been independently observed in *in situ* rat spinotrapezius muscle preparations (7, 35, 49). These observations were later combined to estimate muscle oxygen uptake dynamics following the onset of, and in recovery from, muscle contractions (5, 6). While these studies provide valuable insight into the mechanisms behind skeletal muscle oxygen uptake, limitations exist. The measurements of microvascular hemodynamics and oxygen pressure were collected at a single, relatively low, contraction intensity and were unable to be collected simultaneously in the same muscle preparation, or at moderate-to-severe contraction intensities. Further, the invasive nature of these techniques does not allow them to be directly translated into a human research model.

Near-infrared spectroscopy (NIRS) has been used to noninvasively observe the oxygenation characteristics of exercising skeletal muscle (9, 19, 20, 23, 27, 28, 36, 37, 42, 72). Plateaus in muscle oxygenation measurements using NIRS have been observed during incremental cycling exercise (13, 24, 50). The lack evidence for increases in measurements related to determinants of perfusive and diffusive oxygen delivery suggests an upper limit to

oxygen delivery prior to a maximal work rate (13). Plateaus in muscle oxygenation also appear to be muscle specific, as it has been observed to occur in some, but not all, of muscle in the quadriceps (24). These differences in muscle oxygenation patterns among muscles have been related to differences in fiber-type recruitment patterns (24, 50).

More recently, NIRS has been used in combination with a tracer dye, indocyanine green (ICG), to quantify muscle microvascular blood flow during exercise in humans (15-17, 41, 76). In order to calculate absolute tissue blood flow, NIRS-ICG methodology requires arterial blood sampling for the continuous measurement of ICG concentration (15-17). To circumvent this invasive requirement, an algorithm has recently been developed to estimate relative tissue perfusion and calculate a blood flow index (ICG-BFI) using only the appearance of ICG as detected by NIRS following the venous injection, making the technique less invasive (41). In contrast to the well-established linear relationship between limb blood flow and exercise intensity, both absolute and relative NIRS-ICG methods have demonstrated plateaus in tissue microvascular blood flow at submaximal work intensities (15, 41, 76). The occurrence of a plateau in tissue blood flow would potentially have significant consequence in our current paradigm of oxygen delivery and exercise tolerance at higher exercise intensities.

The physical properties of light employed by NIRS technology to assess tissue oxygenation have been utilized in the development of diffuse correlation spectroscopy (DCS) (11, 12, 31). The movement of light scatterers cause temporal intensity fluctuations in reflected speckle patterns of coherent light sources. DCS measures these temporal intensity fluctuations within reflected near-infrared light patterns caused specifically by the movement of RBCs within tissue (11, 12, 31, 79). As such, DCS provides a noninvasive estimate of tissue microvascular blood flow as a blood flow index (BFI). DCS measurements of BFI have been validated with

several well established methods for measuring blood flow including laser Doppler flowmetry (30), Doppler ultrasound (21, 69), arterial-spin labeled (22, 80) and phase contrast MRI (46), and fluorescent microsphere (81) measurements at rest in both cerebral and skeletal muscle microcirculations. Further, cerebral blood flow measurements made with DCS have demonstrated a strong correlation, and a near 1-to-1 ratio, with measurements made with the NIRS-ICG technique (29). These studies demonstrate that BFI measured using DCS is reliable at rest; however, DCS is highly susceptible to artifact which poses a challenge to its application to skeletal muscle during exercise (10, 71). Still, the potential noninvasive assessment of skeletal muscle tissue blood flow warrants further investigation into the feasibility of using this technology during exercise.

The noninvasive simultaneous measurement of tissue oxygenation (NIRS) and microvascular hemodynamics (DCS) during exercise would provide unique insight into the mechanisms which determine tissue oxygen delivery and utilization. To our knowledge, only one previous study combined NIRS and DCS measurements during exercise, however movement artifacts led to unrealistic blood flow estimates (79). Therefore, the aims of this study were to 1) develop an exercise protocol in which movement artifact was minimized so as to determine if DCS could be used to quantify relative changes in tissue blood flow during exercise intensities ranging from rest to peak work rate, 2) compare DCS-derived BFI of the flexor digitorum superficialis (BFI_{FDS}) muscle to brachial artery blood flow ($\dot{Q}_{BA}$) measured via Doppler ultrasound, and 3) simultaneously measure perfusive and diffusive oxygen transport within a single volume of exercising skeletal muscle tissue. We hypothesized that 1) exercising $\dot{Q}_{BA}$ would increase with increasing exercise intensity until task failure, but 2) based on data from NIRS- ICG protocols, the DCS-derived BFI_{FDS} would plateau at a submaximal work rate. In

addition, we hypothesized that 3) muscle oxygenation characteristics measured with NIRS would demonstrate a plateau at a similar work rate to the hypothesized plateau in BFI_{FDS}. We chose to test these hypotheses in a forearm model of incremental exercise to minimize the relative contribution of subcutaneous adipose tissue and cutaneous circulation to the NIRS and DCS signals.

Chapter 2 - Methods

Twelve men and four women (Mean ± SD; 23.3 ± 3.9 yrs; 170.8 ± 1.9 cm; 72.8 ± 3.4 kg) volunteered to participate in this study. No attempt was made to control for stages of the menstrual cycle in the women. Previous studies showed that muscle blood flow during exercise is not modulated by the menstrual cycle (52, 73). A medical health history evaluation was completed by each subject to confirm the absence of any known cardiovascular or metabolic disease. All experimental procedures were approved by the Institutional Review Board of Kansas State University and conformed to the standards set forth by the Declaration of Helsinki. Subjects were informed of all testing procedures and potential risks of participation prior to providing written informed consent. Subjects were instructed to abstain from vigorous activity 24 h prior, and caffeine or food consumption 2 h prior, to the scheduled testing time.

Experimental design

Each subject performed an incremental handgrip exercise test to task failure on a previously described, custom-built handgrip ergometer (20), which had been modified for single-arm exercise. Briefly, the handle of the ergometer was attached to a pneumatic cylinder by a cable and allowed a fixed linear displacement of 4 cm. Resistance was set by pressurizing the pneumatic cylinder and work was accomplished by compressing the air within the cylinder when the handle was moved. Power output was calculated as $P = Rdf \cdot k^{-1}$, where P is power in Watts (W), R is resistance in kg, d is displacement in meters, f is contraction frequency, and k is the constant 6.12 for the conversion of $kg \cdot m \cdot min^{-1}$ to W. Alterations in power output were accomplished via alterations in resistance (air pressure), as d and f were held constant.

Subjects lay in the supine position with the exercising arm outstretched perpendicular to the body. Two minutes of rest were followed by a three minute warm-up at 1W to establish an exercising baseline. Each stage thereafter, the power was increased by 1 W every two minutes until task failure. Task failure was determined as the inability of the subject to displace the handle of the ergometer the full 4 cm for three consecutive contraction cycles. Peak power (P_{peak}) was determined as the power output during the final stage of exercise lasting a minimum 30s in duration. To eliminate any motion artifact within the DCS measurements, subjects were instructed to remain completely still during the final 10 s of each exercising stage. Previous observations by Lutjemeier et al. (55) found no differences between limb blood flow during exercise and during the first four cardiac cycles following the final contraction of exercise. These findings were subsequently confirmed in the current study. Exercise was performed using a 50% contraction duty cycle (1.5 s contraction: 1.5 s relaxation) at a rate of 20 contractions per minute. An audio recording provided feedback to the subject so that contraction and relaxation timing remained consistent.

Measurements

Doppler ultrasound

Brachial artery mean blood velocity (V_{mean}) and vessel diameter were measured simultaneously using a two-dimensional Doppler ultrasound system (Logiq S8; GE Medical Systems, Milwaukee, WI). The ultrasound system was operated in duplex mode with a phased linear array transducer probe operated at an imaging frequency of 10.0 MHz. To avoid the bifurcation of the brachial artery, all measurements were made 2-5 cm proximal to the antecubital fossa (1). All Doppler velocity measurements were performed at a Doppler frequency

of 4.0 MHz and corrected for an angle of insonation less than 60°. V_{mean} was defined as the time-averaged mean velocity across each complete cardiac cycle. Brachial artery vessel diameter was analyzed at a perpendicular angle along the central axis of the vessel. Cross-sectional area (CSA) of the vessel was then calculated as CSA = πr^2. Limb blood flow ($\dot{Q}_{BA}$) was calculated during the 10s end-stage resting period during the protocol as the product of CSA and V_{mean}.

Near-infrared and diffuse correlation spectroscopies

A system equipped to simultaneously employ frequency-domain multidistance NIRS and DCS was used to measure oxygenation characteristics and BFI_{FDS} during handgrip exercise (MetaOx, ISS, Champaign, IL, USA). A NIRS system (Oxiplex TS, ISS, Champaign, IL, USA) has been utilized previously by our laboratory to characterize the oxygenation of skeletal muscle (19, 20, 34, 36, 72). This previously used system consisted of eight laser diodes operating at wavelengths of 690 and 830 nm (4 laser diodes per wavelength) with one detector fiber bundle and detector separation distances of 2.0, 2.5, 3.0, and 3.5 cm. The NIRS component of the dual spectroscopy (NIRS and DCS) system used in the current study consisted of eight laser diodes operating at wavelengths of 660, 690, 705, 730, 760, 785, 810, 830 nm with power outputs of 5-9 mW. Four detector fiber bundles were positioned with detector separation distances of 2.5, 3.0, 3.5, and 4.0 cm, allowing for an estimated tissue penetration depth of 2.0 cm, approximately half of the maximal separation distance.

The NIRS system measures and incorporates the dynamic reduced scattering coefficients (μ_s') to provide absolute concentrations (μM) for deoxygenated [Hb+Mb] (deoxy-[Hb+Mb]), oxygenated [Hb+Mb] (oxy-[Hb+Mb]), total-[Hb+Mb], and % saturation (oxy-[Hb+Mb]×100/total-[Hb+Mb]). Changes in total-[Hb+Mb] are thought to reflect changes in microvascular hematocrit (an index of diffusive conductance) (25, 62). Changes in deoxy-

[Hb+Mb] concentrations have been used to estimate fractional oxygen extraction (an index of perfusive conductance) (19, 20, 26-28, 33, 34, 37, 56). The principles and algorithms of the NIRS technology have been reviewed by Gratton et al. (39) and were previously described by Ferreira et al. (34). The original deoxy-[Hb+Mb], oxy-[Hb+Mb], and total-[Hb+Mb] concentrations were multiplied by a factor of four to convert from units of hemoglobin concentration into units of heme concentrations and are hereby denoted as deoxy-[heme], oxy-[heme], and total-[heme], respectively.

DCS measures temporal intensity fluctuations in a reflected near-infrared light pattern, caused primarily by moving RBCs (11, 12, 79), to provide a microvascular BFI in units of cm^2/s. The correlation equations and algorithms used for DCS have been described in detail by Durduran et al. (31). Relative changes in BFI have been used to quantify relative changes in cerebral and skeletal muscle tissue blood flow (29, 32, 46, 53, 79-81). The DCS module of the dual spectroscopy system used in the current study was comprised of four photon-counting photodiode detectors located 3.1 cm from a single, long coherence length, laser diode operating at a wavelength of 850 nm with an intensity of 50 mW. Tissue penetration depth of the DCS probe is estimated as half of the laser-detector serperation distance (~1.5 cm). All components of the NIRS and DCS system were housed within the same sensor so that measures of tissue oxygenation and BFI could be made of the same volume of tissue.

The belly of the FDS was located using electromyography (EMG) and tissue palpations as previously described (20). The NIRS/DCS sensor was secured over the belly of the FDS and wrapped with an elastic bandage to prevent movement of the sensor and to prevent any ambient light from reaching the detectors. NIRS and DCS measurements were collected at 10 Hz during the entire experimental protocol. Tissue oxygenation measurements using NIRS were averaged

during resting baseline and the final 10s of exercise during each stage of the protocol. BFI_{FDS} measurements were averaged during the 10s end-stage resting period i.e., during the 10s subsequent to the 10s window used for NIRS measurements (Figure 2).

Statistical analysis

Statistical analysis was performed using SigmaStat (Systat Software, Point Richmond, CA). Data are expressed as mean ± SD unless otherwise noted. $\dot{Q}_{BA}$ and the NIRS/DCS variables (BFI, total-[heme], deoxy-[heme], and % saturation) were compared across work rates using a one-way repeated measures analysis of variance (ANOVA). To identify differences between $\dot{Q}_{BA}$ and BFI_{FDS}, data were expressed as a percent change from resting baseline and compared using a two-way repeated measures ANOVA (measurement × work rate). When a significant overall effect was detected, a Tukey's post hoc analysis was performed to determine where significant differences existed. Statistical significance was defined as $p < 0.05$ for all analyses. Finally, a plateau was considered present in a response when a minimum of two consecutive work rate transitions elicited no significant increase and the value of the signal was not different than at P_{peak}.

Chapter 3 - Results

The average P_{peak} achieved by subjects was 6.2 ± 1.4W with P_{peak} ranging from 4 to 8W. Figure 1 provides the raw signals of BFI_{FDS}, total-[heme], and deoxy-[heme] measured using the combined NIRS/DCS system of a single representative subject during the entire experimental protocol. Figure 2 provides detail of the raw BFI_{FDS}, total-[heme], and deoxy-[heme] signals of the same representative subject during an exercise-rest-exercise transition during the experimental protocol.

The responses of $\dot{Q}_{BA}$ and BFI_{FDS} from rest to 3W and at P_{peak} are illustrated in Figures 3A and 3C, respectively. $\dot{Q}_{BA}$ was greater at P_{peak} (617 ± 271 ml/min) than at work rates from rest to 3W ($p < 0.001$). Likewise, BFI_{FDS} was greater at P_{peak} (1.91 ± 1.42 $cm^2/s \times 10^{-8}$) than at work rates from rest to 3W ($p < 0.05$). However, the wide range in P_{peak} among subjects resulted in a discrepancy in the submaximal-to-maximal work rate difference from which end-exercise comparisons were made. For example, a subject having achieved the highest observed P_{peak} (8W) demonstrates a 5W difference between P_{peak} and the highest submaximal work rate achieved by all subjects (3W). A subject having achieved the lowest observed P_{peak} (4W) demonstrates only a 1W difference between P_{peak} and 3W. Therefore, in order to compare any changes in $\dot{Q}_{BA}$ or BFI_{FDS} between work rates immediately preceding the final stage of exercise, the 3 work rates preceding P_{peak} (P_{peak-3}, P_{peak-2}, P_{peak-1}) as well as P_{peak} were compared and presented in Figures 3B and 3D.

The average exercise intensity at P_{peak-2} was 65.8 ± 8.26% of P_{peak}. $\dot{Q}_{BA}$ increased with increases in work rate from P_{peak-3} to P_{peak-1} ($p < 0.05$). However, no significant difference was detected in $\dot{Q}_{BA}$ between P_{peak-1} and P_{peak} ($p = 0.38$). BFI_{FDS} did not increase with work rate at

any intensity greater than P_{peak-2}, demonstrating a submaximal plateau (Figure 3D), in contrast to the visual implication inferred in Figure 3C. In addition, the percent increase from rest in $\dot{Q}_{BA}$ was greater than the percent increase from rest in BFI_{FDS} at P_{peak-1} and P_{peak} ($p < 0.05$) (Figure 4).

The average changes in total-[heme], deoxy-[heme], and % saturation from rest to 3W and at P_{peak} are illustrated in Figures 5A-5C. Total-[heme] and deoxy-[heme] concentrations increased with exercise intensity ($p < 0.001$) while % saturation decreased with increases in exercise intensity ($p < 0.001$). As described previously with regard to $\dot{Q}_{BA}$ and BFI_{FDS}, average total-[heme], deoxy-[heme], and % saturation for the 3 work rates preceding P_{peak} (P_{peak-3}, P_{peak-2}, P_{peak-1}) as well as P_{peak} were compared and presented in Figures 5D-5F. Total-[heme] at P_{peak} and P_{peak-1} was greater than total-[heme] at P_{peak-3} ($p < 0.001$). Deoxy-[heme] and % saturation were greater at P_{peak} than at P_{peak-3} ($p < 0.05$). However, there were no differences in total-[heme], deoxy-[heme], or % saturation between succeeding exercise intensities from P_{peak-2} to P_{peak} suggesting a plateau in the responses.

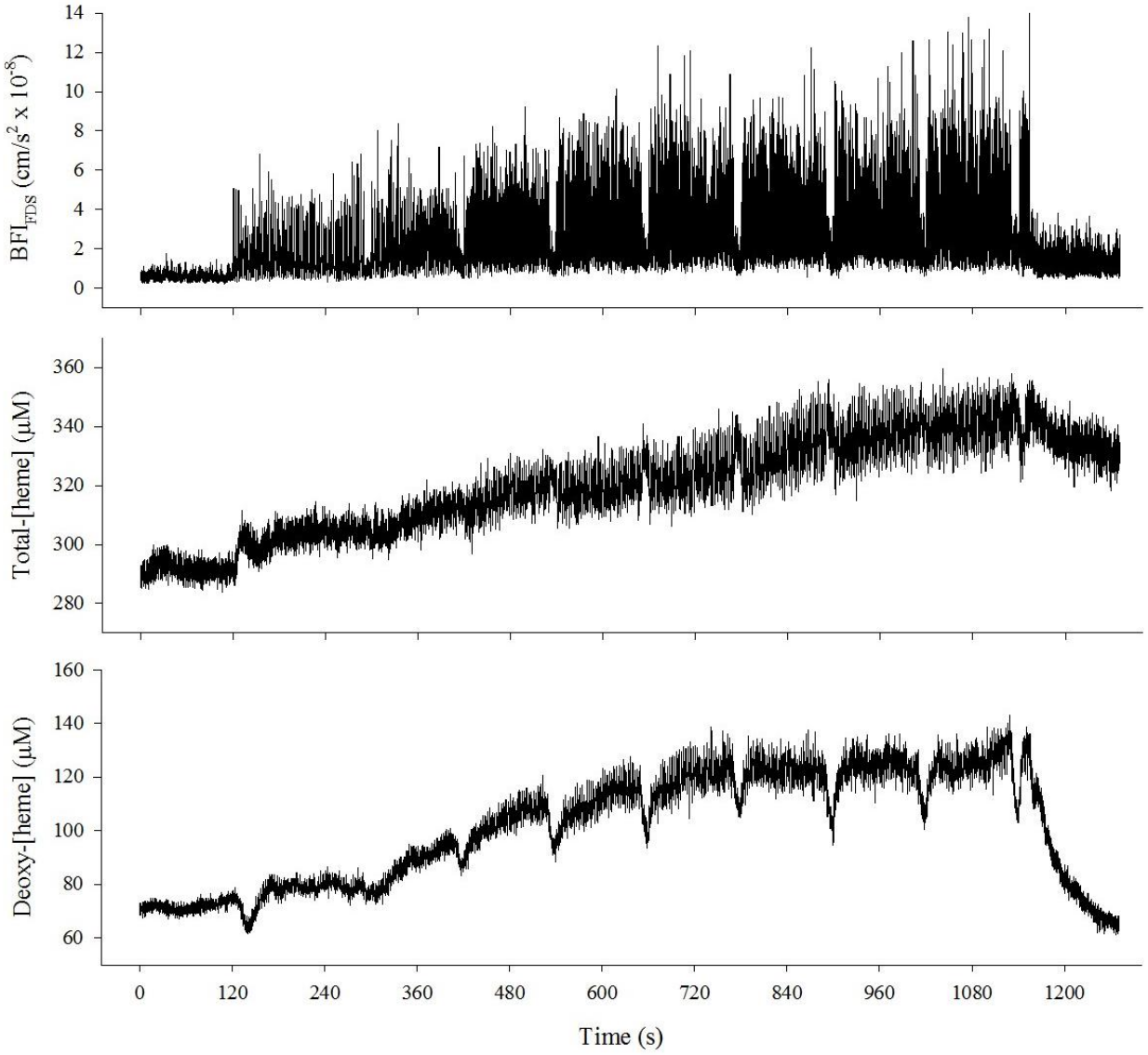

Figure 1. Raw diffuse correlation and near-infrared spectroscopy signals

BFI_{FDS} (top), total-[heme] (middle), and deoxy-[heme] (bottom) signals of a single representative subject through the entire incremental handgrip exercise test performed to task failure. Note the large amount of motion artifact in the BFI_{FDS} signal during muscular contractions (top).

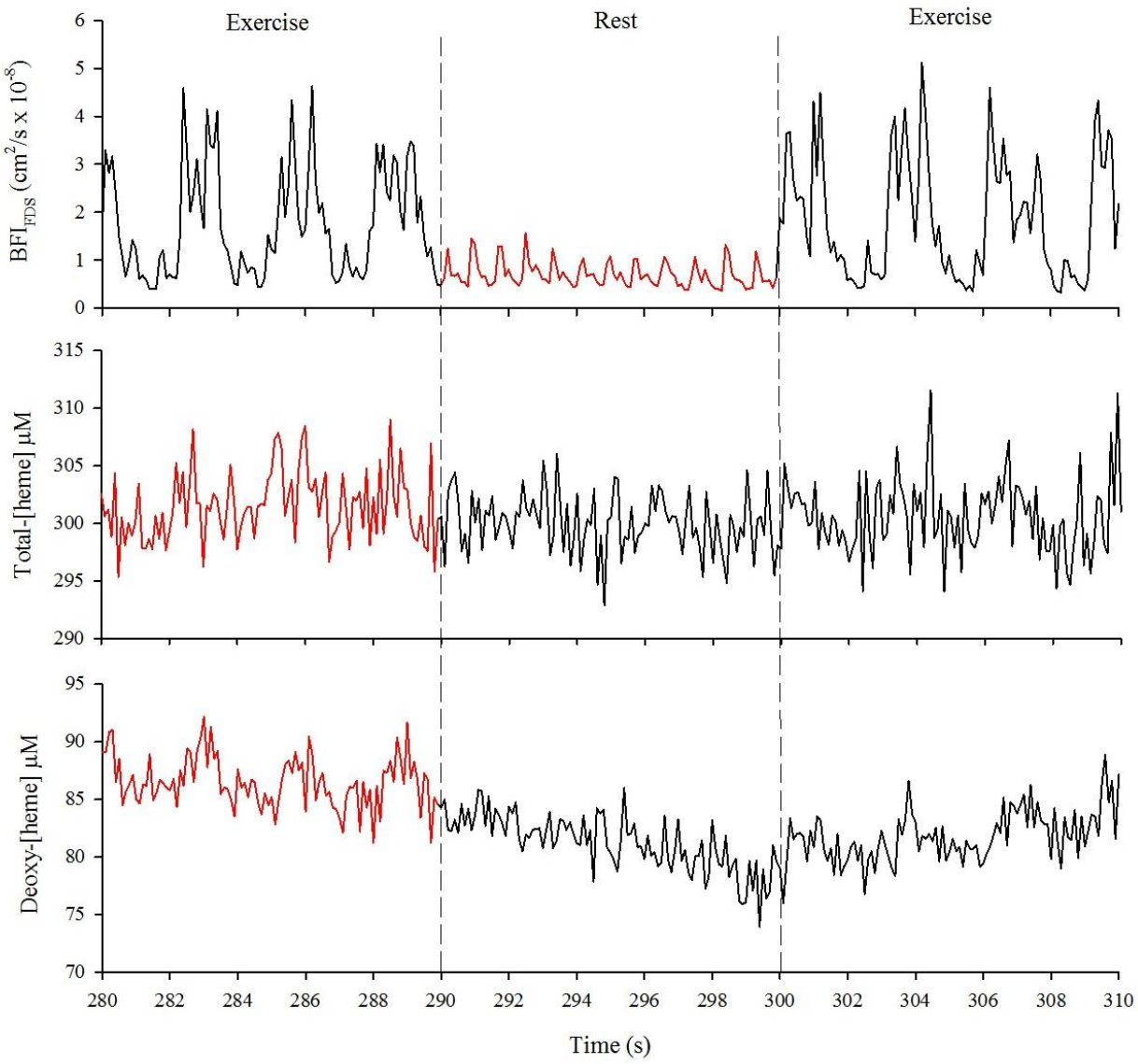

Figure 2. Detailed diffuse correlation and near-infrared spectroscopy signals

Detailed figure of the raw BFI_{FDS}, total-[heme], and deoxy-[heme] signals during an exercise-rest-exercise transition of the same subject represented in Figure 1. Highlighted portions in red indicate the time interval of data analysis for each respective signal. Note the lack of reduction in the BFI_{FDS} signal between the relaxation phases of contractions and the 10s end-stage resting period.

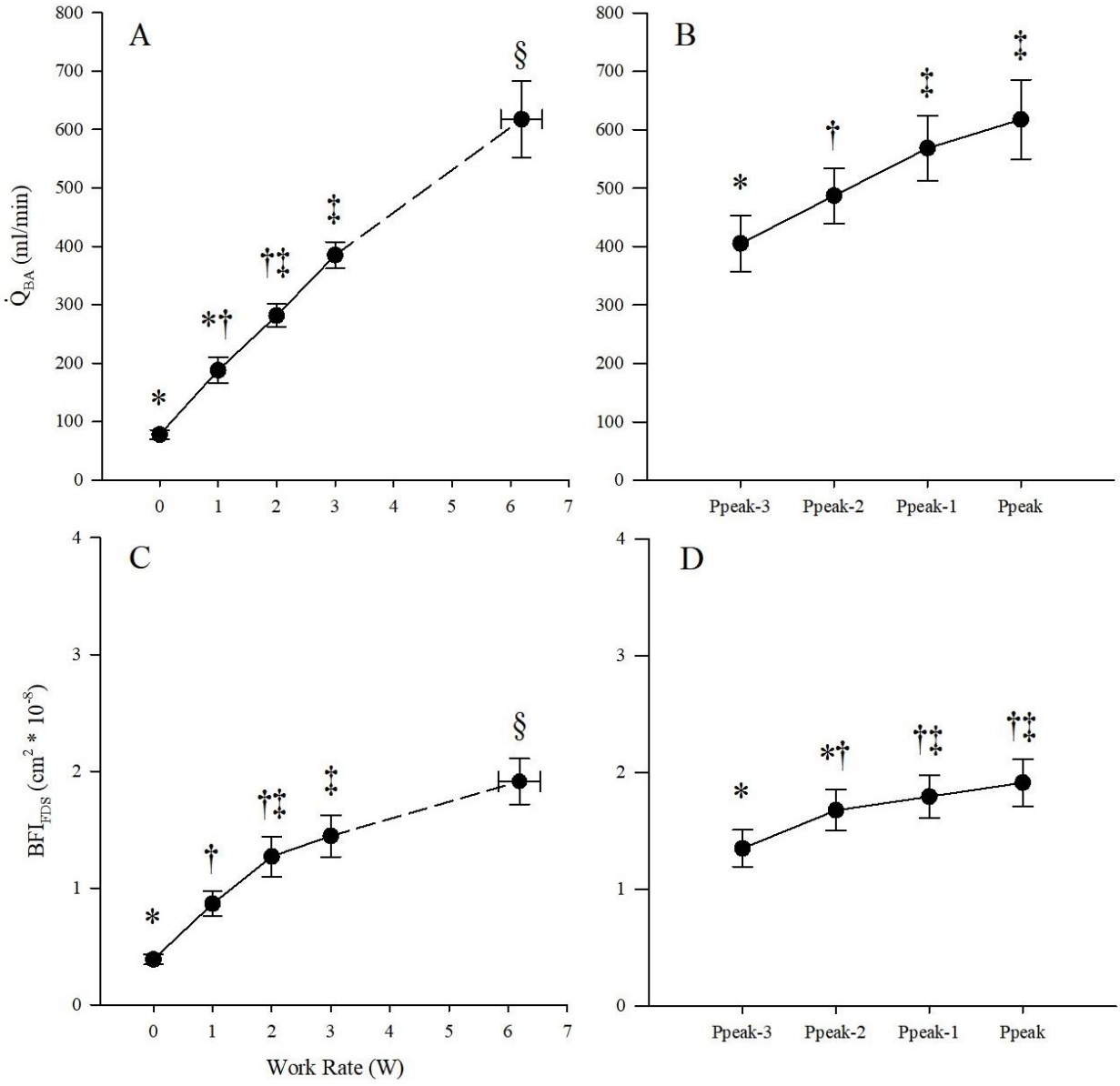

Figure 3. Bulk conduit artery and microvascular hemodynamic responses

Mean responses for $\dot{Q}_{BA}$ (top) and BFI_{FDS} (bottom) from rest to P_{peak} (left) and from P_{peak-3} to P_{peak} (right) during the incremental hand grip exercise test performed until task failure. Shared symbols indicate no significant difference between/among work rates ($p > 0.05$). Note that no increase was observed in BFI_{FDS} beyond P_{peak-2} (D).

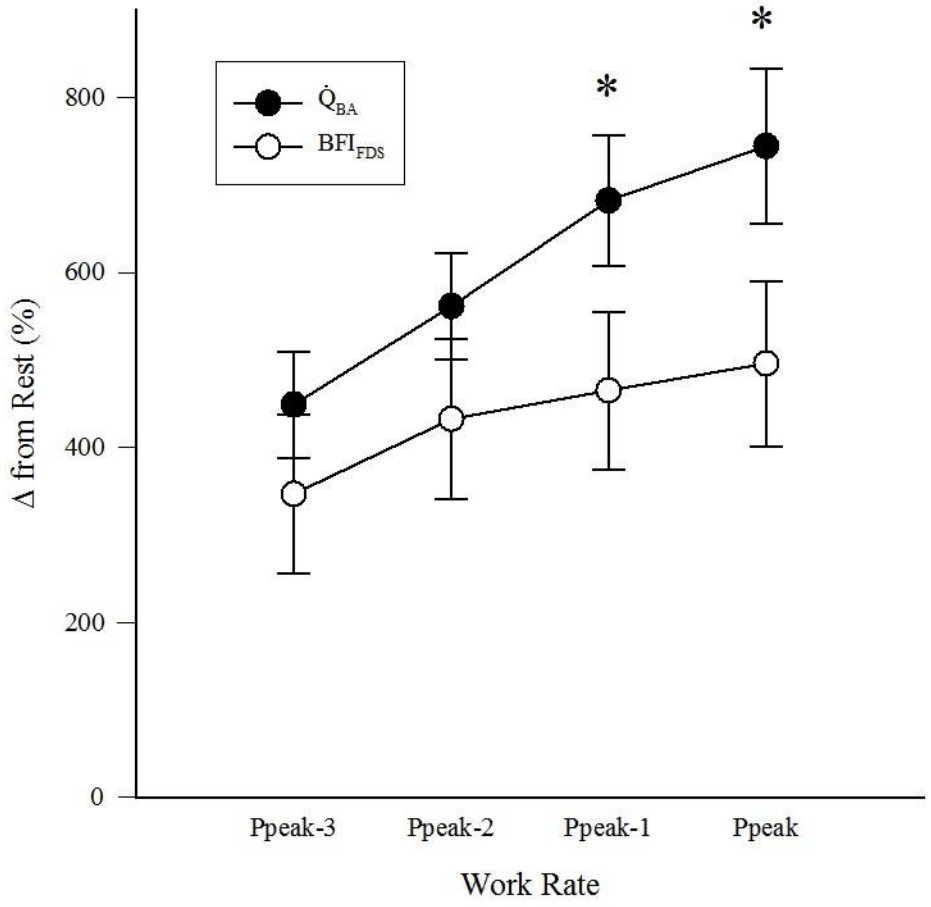

Figure 4. Percent change in conduit artery and microvascular hemodynamics

Bulk conduit artery and microvascular hemodynamic responses to the incremental hand grip exercise as a percent change from rest. The mean percent change from rest for $\dot{Q}_{BA}$ (●) and BFI_{FDS} (○) from P_{peak-3} to P_{peak}. *Significantly greater than BFI_{FDS} ($p < 0.05$).

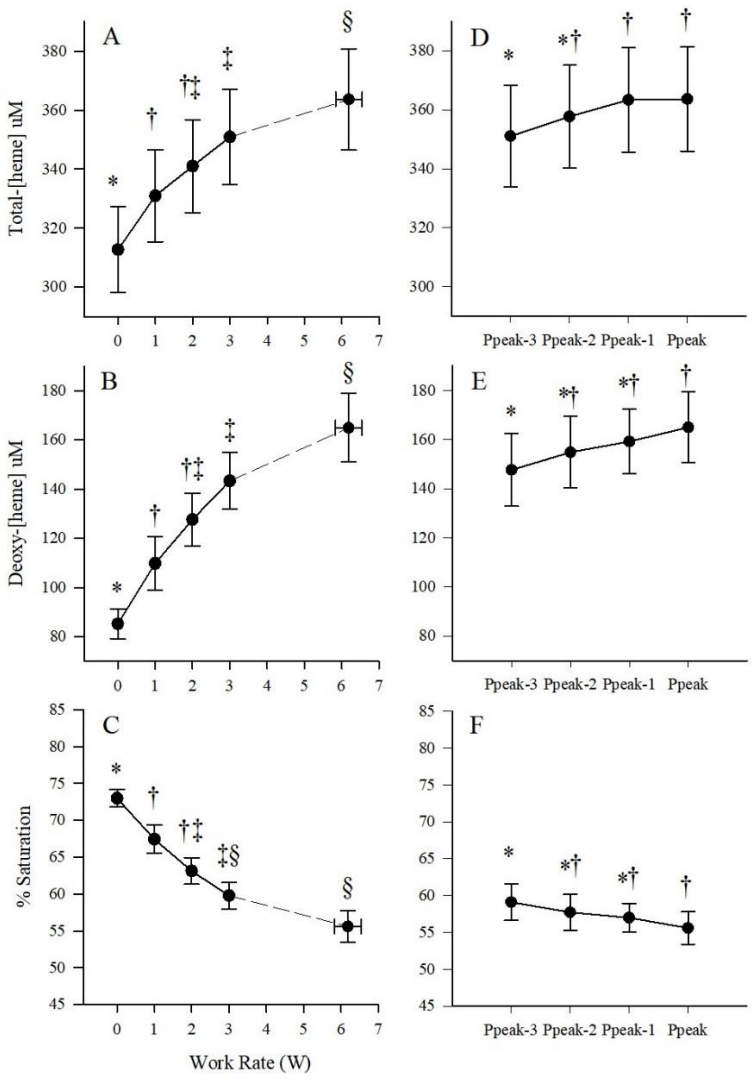

Figure 5. Muscle oxygenation responses

The mean responses for total-[heme] (top), deoxy-[heme] (middle), and % saturation (bottom) from rest to P_{peak} (left) and from P_{peak-3} to P_{peak} (right) during the incremental hand grip exercise test performed until task failure. Shared symbols indicate no significant difference between/among work rates ($p > 0.05$). Note that no increases were observed in any of the NIRS measurements beyond P_{peak-2}.

Chapter 4 - Discussion

This study examined the responses of conduit artery blood flow and skeletal muscle hemodynamics during incremental forearm exercise. As has been demonstrated previously (2, 67), and in agreement with of our first hypothesis, $\dot{Q}_{BA}$ increased with exercise intensity until the final work rate transition (Figure 3B). In contrast, BFI_{FDS} plateaued at a submaximal work rate (P_{peak-2}) (Figure 3D), consistent with previous findings using NIRS-ICG (15, 41, 76) and our second hypothesis. In addition, muscle oxygenation characteristics (total-[heme], deoxy-[heme], and % saturation) measured with NIRS demonstrated a plateau at the same work rate as BFI_{FDS} measured with DCS (Figures 5D-5F). Importantly, the perfusive (BFI_{FDS} and deoxy-[heme]) and diffusive (total-[heme]) measurements of oxygen transport were collected simultaneously during exercise within the same volume of tissue.

Diffuse correlation spectroscopy signal analysis

A considerable amount of motion artifact existed in the BFI_{FDS} signal during exercise (Figure 1). The protocol implemented during the present study allowed BFI_{FDS} to be collected with little to no motion artifact present, without compromising the integrity of the measurement, i.e., no reductions in the BFI_{FDS} signal were observed between the final relaxation phases of contractions and the 10s end-stage resting periods (Figure 2). This observation allowed for confidence in the BFI measurements of the current study, specifically, to their physiological significance to microvascular hemodynamics during exercise. Further, this observation is consistent with the findings of Lutjemeier et al. (55) who found no differences between limb

blood flow during exercise and in the first four cardiac cycles of early recovery and provides detailed rational for this approach.

Comparison of hemodynamic responses to exercise

Increases in exercise intensity were met with appropriate increases in $\dot{Q}_{BA}$ (Figures 3A and 3B) to increase oxygen supply to the working skeletal muscles. However, BFI_{FDS} did not increase beyond $P_{peak\text{-}2}$ (~66% of P_{peak} on average) (Figure 3D). These findings are consistent with studies using the NIRS-ICG methods for muscle blood flow assessment during incremental exercise in muscles of the thigh (15, 41, 76). Although NIRS-ICG and DCS share the employment of near-infrared light, these techniques determine muscle blood flow through measurement of very different physiological phenomena.

ICG is a florescent dye that binds to plasma proteins and is used as an additional light absorber within the microcirculation. The appearance of a reduction in the NIRS signal can be attributed to the movement of ICG through the microcirculation allowing for the calculation of tissue blood flow. In contrast to the NIRS-ICG technique, DCS measures temporal intensity fluctuations in near-infrared light caused directly by the movement of light scatterers (primarily RBCs) (11, 12, 79). Changes in the frequency and amplitude of intensity fluctuations can be used to quantify relative changes in microvascular blood flow as a BFI. Thus, the observation of a submaximal plateau in microvascular muscle blood flow using two unique measurement techniques, which reflect different components of whole blood, provides additional confidence as to its occurrence. Further, the submaximal plateau in microvascular muscle blood flow has now been observed in muscles of the forearm (present study) and of the thigh (15, 41, 76), suggesting a common physiological phenomenon across muscle groups.

We speculate the disconnect between increases in $\dot{Q}_{BA}$ and BFI_{FDS} can be explained by differences in muscle activation, and therefore oxygen demand, among finger and wrist flexor skeletal muscles as exercise intensity was increased. It is likely that the FDS, the muscle primarily responsible for finger flexion, is recruited proportionally more during handgrip exercise performed at lower work rates; hence the initial matching of BFI_{FDS} to increases in work rate (Figure 3C). However, as exercise intensity increases, other finger and wrist flexor muscles were likely recruited to meet the force requirements of the exercise. The recruitment of additional muscles or greater activation of already contributing ones, would require an increase in $\dot{Q}_{BA}$ to increase total oxygen supply to the whole limb.

Heterogeneity of muscle blood flow within and among exercising skeletal muscles has been demonstrated numerous times in both animals (3, 45, 50, 51, 60, 61, 64) and humans (43, 44, 47, 48, 50). The distribution of blood flow within and among synergistic muscle groups permits closer matching of oxygen delivery to the specific oxygen demands of individual motor units. Closer matching of oxygen supply and demand facilitates the maintenance of a sufficient oxygen pressure gradient required for diffusive oxygen delivery from the microvasculature to the muscle (58, 77, 78). As exercise intensity increases, blood flow heterogeneity within a muscle group decreases (44). This observation reflects the distribution of increases in blood flow toward newly recruited motor units as exercise intensity progresses (66). Thus, if the FDS was maximally activated at submaximal work rates, we would not expect to see an increase in oxygen delivery to that muscle with further increases in work rate.

Noninvasive oxygen transport measurements

In the present study, optical spectroscopy techniques employing near infrared light allowed both perfusive (BFI_{FDS} and deoxy-[heme]) and diffusive (total-[heme]) oxygen transport to be measured noninvasively in a single volume of tissue during exercise (Figures 1 & 2). These measurements are required, in concert, to assess muscle oxygen consumption. Many innovative techniques for measuring individual components of oxygen delivery have been previously developed for use in animal models; notably, microscopy (49, 68, 70) and radiolabeled microspheres (3, 4, 45, 51) for measurements of microvascular hemodynamics and tissue blood flow, respectively, and phosphorescent quenching for measurements of changes in microvascular oxygen pressures (indicative of oxygen extraction) (7, 8, 57). These techniques have provided fundamental insights into muscle metabolism during rest and exercise but are extremely invasive and can be used with only mild contraction intensities, and thus are not suited for research in humans.

In humans, NIRS has allowed for noninvasive measurement of diffusive (total-[Hb+Mb]) (25, 62) and perfusive oxygen conductance (deoxy-[Hb+Mb]) (19, 20, 27, 28, 36) within skeletal muscle. However, measurement of blood flow at the level of tissue gas exchange has remained fairly evasive. The combination of DCS and NIRS, as employed by this study, to measure perfusive and diffuse oxygen transport across exercise intensities, is a unique approach to potentially assess oxygen consumption of exercising skeletal muscles. Importantly, this technique is completely noninvasive and allows for measurements to be made simultaneously during exercise.

Plateaus in the NIRS signals observed during this study have been reported previously during cycling exercise (13, 63, 74). Changes in total-[heme] are reflective of changes in

microvascular hematocrit, a primary determinant of diffusive microvascular oxygen delivery (25, 62). Changes in deoxy-[heme] are reflective of microvascular oxygen extraction and indicate changes in perfusive microvascular oxygen delivery (19, 20, 27, 28, 36).The observation of plateaus in BFI_{FDS} and deoxy-[heme] (indices of perfusive oxygen conductance), and total-[heme] (an index of diffusive oxygen conductance) at the same submaximal work rate (P_{peak-2}) suggests similar mechanisms leading to a potential upper limit in both the diffusive capacity and delivery for microvascular oxygen uptake. Further, the identification of discrepancies in the patterns of increase in muscle oxygenation characteristics (total-[Hb+Mb] and deoxy-[Hb+Mb]) among muscles within the quadriceps during incremental cycling exercise (24, 63) emphasizes the need for further investigation of oxygen characteristics as they relate to muscle activation patterns during incremental exercise.

Laughlin and Armstrong observed differences in the blood flow responses among, and within, the exercising skeletal muscles of rats during treadmill running (51). The variability in blood flow responses were attributed, in part, to differences in muscle fiber type and recruitment patterns. Additionally, it was noted that differences in blood flow responses among, and within, muscles were magnified with increased exercise intensity. These observations compliment the findings of the current study in that plateaus were similarly observed in individual muscles of a limb while exercise intensity was increased.

Limitations

Appropriate interpretation of the data from this study requires the acknowledgement of several limitations. The NIRS/DCS probe was placed on the forearm prior to exercise and was not removed until exercise had ceased. While this was advantageous in assuring a single volume

of tissue was interrogated during the testing protocol, it presents the question of reproducibility of the NIRS/DCS signals. Location of the FDS muscle was confirmed using EMG, as has been done previously in our lab (19, 20). However, it is possible that other finger and wrist flexor muscles contributed to the overall NIRS-DCS signals, especially at higher power outputs. Contributions from muscles other than the FDS to the power output of the whole limb would pose a challenge to the interpretation of both the BFI_{FDS} signal and any NIRS-derived measurements.

EMG was not collected during the exercise protocol. The single-arm handgrip mode of exercise only allowed for placement of one measurement probe (NIRS/DCS) over the targeted area of the forearm (FDS). Therefore, conclusions made of relative changes in tissue blood flow during incremental exercise related to muscle recruitment patterns are only speculative. However, subjects were observed engaging wrist flexion during the later stages of the exercise test, as opposed to finger flexion alone. This observation requires confirmation with EMG. However, it has been demonstrated that muscles are recruited in a non-linear fashion during incremental forearm exercise (59). Further, during incremental cycling exercise, muscles of the quadriceps demonstrated markedly different deoxy-[Hb+Mb] (an index of perfusive oxygen delivery) responses which were directly related to differences in muscle recruitment patterns (24). These differences in muscle contribution between work rates could be due to differences in fiber-type recruitment patterns and mechanical efficiencies among these muscles.

DCS and NIRS measurements are entirely noninvasive. The indirect nature of these measurements permits influence, to some degree, by other tissues such as the skin and subcutaneous adipose tissue. In particular, the strength of the optical spectroscopic signals are influenced by adipose tissue thickness and accuracy of probe placement (14, 18, 75). Further, the

relative contribution of arterioles, venules and capillaries to the optical signals across exercise intensities is not clear and pose question to their validity as measures of purely microvascular oxygen transport. However, capillaries comprise the majority of the muscle microvascular volume (65) and, therefore, changes in the optical signals likely represent changes in the respective oxygen transportation measurements at this level of the microcirculation (34, 54).

Previously, absolute values of muscle oxygen uptake ($m\dot{V}O_2$) have been estimated using $\dot{Q}_{BA}$ and deoxy-[Hb+Mb] during handgrip exercise (20). However, the DCS technique does not provide absolute quantification of tissue blood flow as has been accomplished through several other more invasive techniques such as radiolabeled microspheres (3, 4, 45, 51) or microscopy (49, 68, 70) in animals and NIRS-ICG (15, 17, 41, 76) in humans. Therefore, at the present time, changes in BFI can only be interpreted as relative changes in tissue blood flow from a resting baseline signal. As such, estimates of absolute $m\dot{V}O_2$ using purely microvascular oxygen delivery measurements were unable to be made.

The BFI signal is a result of the movement of RBCs relative to the DCS light detector. At rest, the detector remains still, therefore, any signal is the result of RBC movement in the field of view of the DCS probe. Note the fidelity of the BFI signal at rest (Figure 2), even to the point of demonstrating a notch in the waveform similar to the dicrotic notch observed in the arterial pressure waveform. However, during exercise movement of the probe in relation to tissues below it causes artifact in the BFI signal. Thus, muscle contraction itself produces substantial noise in the BFI signal and must be accounted for during analysis. Previously, motion artifact in DCS data was successfully reduced during single-intensity dynamic exercise by analyzing DCS data only during the relaxation phase of muscular contraction cycles, through the employment of gating algorithms (40, 71). However, substantial variability in individual responses suggests

some degree of motion artifact remained in the analyzed signals. Further, DCS measurements were constrained to short collection time windows due to either low DCS sampling frequencies (71) or relatively short relaxation times (40).

The protocol of the current study allowed for motion-artifact-free DCS measurements by only analyzing the signals during the 10s end-stage resting period (Figure 2). This approach allowed for a much longer window of DCS data collection while assuring minimal introduction of motion artifact. It should be noted that the signal analysis of NIRS and DCS measurements were conducted during different time intervals of the protocol (Figure 2). Thus, any conclusions made by the combination of perfusive (BFI_{FDS} and deoxy-[heme]) and diffusive (total-[heme]) oxygen transport measurements may require additional caution. However, these measurements were each analyzed at time intervals that were only 10s apart and which most accurately reflected their values observed during exercise while permitting signals uncompromised by limb movement, i.e., motion-artifact-free BFI_{FDS} data.

Conclusions

DCS was demonstrated to be a powerful, noninvasive tool for quantifying relative changes in microvascular skeletal muscle blood flow during incremental handgrip exercise. Strategic experimental methodology was incorporated to minimize complications due to the susceptibility of DCS for motion artifact. While $\dot{Q}_{BA}$ increased linearly with exercise intensity, perfusive (BFI_{FDS} and deoxy-[heme]) and diffusive (total-[heme]) oxygen transport measurements of the FDS plateaued at a common submaximal work rate. Further studies are required to investigate whether muscle recruitment differences amongst muscles of the whole limb can explain the discrepancies observed in $\dot{Q}_{BA}$ and BFI_{FDS} responses during incremental

exercise. Finally, future studies employing DCS should aim to challenge oxygen delivery to skeletal muscles to further solidify the utility of DCS for robust investigation of muscle microvascular blood flow responses to exercise.

References

1. **Ade CJ, Broxterman RM, Wong BJ, and Barstow TJ**. Anterograde and retrograde blood velocity profiles in the intact human cardiovascular system. *Exp Physiol* 97: 849-860, 2012.
2. **Andersen P, and Saltin B**. Maximal perfusion of skeletal muscle in man. *J Physiol* 366: 233-249, 1985.
3. **Armstrong RB, and Laughlin MH**. Exercise blood flow patterns within and among rat muscles after training. *Am J Physiol* 246: H59-68, 1984.
4. **Armstrong RB, and Laughlin MH**. Rat muscle blood flows during high-speed locomotion. *J Appl Physiol (1985)* 59: 1322-1328, 1985.
5. **Behnke BJ, Barstow TJ, Kindig CA, McDonough P, Musch TI, and Poole DC**. Dynamics of oxygen uptake following exercise onset in rat skeletal muscle. *Respir Physiol Neurobiol* 133: 229-239, 2002.
6. **Behnke BJ, Ferreira LF, McDonough PJ, Musch TI, and Poole DC**. Recovery dynamics of skeletal muscle oxygen uptake during the exercise off-transient. *Respir Physiol Neurobiol* 168: 254-260, 2009.
7. **Behnke BJ, Kindig CA, Musch TI, Koga S, and Poole DC**. Dynamics of microvascular oxygen pressure across the rest-exercise transition in rat skeletal muscle. *Respir Physiol* 126: 53-63, 2001.
8. **Behnke BJ, McDonough P, Padilla DJ, Musch TI, and Poole DC**. Oxygen exchange profile in rat muscles of contrasting fibre types. *J Physiol* 549: 597-605, 2003.
9. **Belardinelli R, Barstow TJ, Porszasz J, and Wasserman K**. Changes in skeletal muscle oxygenation during incremental exercise measured with near infrared spectroscopy. *Eur J Appl Physiol Occup Physiol* 70: 487-492, 1995.
10. **Belau M, Ninck M, Hering G, Spinelli L, Contini D, Torricelli A, and Gisler T**. Noninvasive observation of skeletal muscle contraction using near-infrared time-resolved reflectance and diffusing-wave spectroscopy. *J Biomed Opt* 15: 057007, 2010.
11. **Boas DA, Campbell LE, and Yodh AG**. Scattering and Imaging with Diffusing Temporal Field Correlations. *Phys Rev Lett* 75: 1855-1858, 1995.
12. **Boas DA, and Yodh AG**. Spatially varying dynamical properties of turbid media probed with diffusing temporal light correlation. *J Opt Soc Am A* 14: 192-215, 1997.
13. **Boone J, Barstow TJ, Celie B, Prieur F, and Bourgois J**. The impact of pedal rate on muscle oxygenation, muscle activation and whole-body VO(2) during ramp exercise in healthy subjects. *Eur J Appl Physiol* 115: 57-70, 2015.
14. **Bopp CM, Townsend DK, and Barstow TJ**. Characterizing near-infrared spectroscopy responses to forearm post-occlusive reactive hyperemia in healthy subjects. *Eur J Appl Physiol* 111: 2753-2761, 2011.
15. **Boushel R, Langberg H, Gemmer C, Olesen J, Crameri R, Scheede C, Sander M, and Kjaer M**. Combined inhibition of nitric oxide and prostaglandins reduces human skeletal muscle blood flow during exercise. *J Physiol* 543: 691-698, 2002.
16. **Boushel R, Langberg H, Green S, Skovgaard D, Bulow J, and Kjaer M**. Blood flow and oxygenation in peritendinous tissue and calf muscle during dynamic exercise in humans. *J Physiol* 524 Pt 1: 305-313, 2000.
17. **Boushel R, Langberg H, Olesen J, Nowak M, Simonsen L, Bulow J, and Kjaer M**. Regional blood flow during exercise in humans measured by near-infrared spectroscopy and indocyanine green. *J Appl Physiol (1985)* 89: 1868-1878, 2000.
18. **Bowen TS, Rossiter HB, Benson AP, Amano T, Kondo N, Kowalchuk JM, and Koga S**. Slowed oxygen uptake kinetics in hypoxia correlate with the transient peak and reduced spatial distribution of absolute skeletal muscle deoxygenation. *Exp Physiol* 98: 1585-1596, 2013.
19. **Broxterman RM, Ade CJ, Craig JC, Wilcox SL, Schlup SJ, and Barstow TJ**. Influence of blood flow occlusion on muscle oxygenation characteristics and the parameters of the power-duration relationship. *J Appl Physiol (1985)* 118: 880-889, 2015.

20. **Broxterman RM, Ade CJ, Wilcox SL, Schlup SJ, Craig JC, and Barstow TJ**. Influence of duty cycle on the power-duration relationship: observations and potential mechanisms. *Respir Physiol Neurobiol* 192: 102-111, 2014.
21. **Buckley EM, Cook NM, Durduran T, Kim MN, Zhou C, Choe R, Yu GQ, Shultz S, Sehgal CM, Licht DJ, Arger PH, Putt ME, Hurt H, and Yodh AG**. Cerebral hemodynamics in preterm infants during positional intervention measured with diffuse correlation spectroscopy and transcranial Doppler ultrasound. *Opt Express* 17: 12571-12581, 2009.
22. **Carp SA, Dai GP, Boas DA, Franceschini MA, and Kim YR**. Validation of diffuse correlation spectroscopy measurements of rodent cerebral blood flow with simultaneous arterial spin labeling MRI; towards MRI-optical continuous cerebral metabolic monitoring. *Biomed Opt Express* 1: 553-565, 2010.
23. **Chance B, Nioka S, Kent J, Mccully K, Fountain M, Greenfeld R, and Holtom G**. Time-Resolved Spectroscopy of Hemoglobin and Myoglobin in Resting and Ischemic Muscle. *Anal Biochem* 174: 698-707, 1988.
24. **Chin LM, Kowalchuk JM, Barstow TJ, Kondo N, Amano T, Shiojiri T, and Koga S**. The relationship between muscle deoxygenation and activation in different muscles of the quadriceps during cycle ramp exercise. *J Appl Physiol (1985)* 111: 1259-1265, 2011.
25. **Davis ML, and Barstow TJ**. Estimated contribution of hemoglobin and myoglobin to near infrared spectroscopy. *Respir Physiol Neurobiol* 186: 180-187, 2013.
26. **De Blasi RA, Cope M, Elwell C, Safoue F, and Ferrari M**. Noninvasive measurement of human forearm oxygen consumption by near infrared spectroscopy. *Eur J Appl Physiol Occup Physiol* 67: 20-25, 1993.
27. **DeLorey DS, Kowalchuk JM, and Paterson DH**. Effects of prior heavy-intensity exercise on pulmonary O2 uptake and muscle deoxygenation kinetics in young and older adult humans. *J Appl Physiol (1985)* 97: 998-1005, 2004.
28. **DeLorey DS, Kowalchuk JM, and Paterson DH**. Relationship between pulmonary O2 uptake kinetics and muscle deoxygenation during moderate-intensity exercise. *J Appl Physiol (1985)* 95: 113-120, 2003.
29. **Diop M, Verdecchia K, Lee TY, and St Lawrence K**. Calibration of diffuse correlation spectroscopy with a time-resolved near-infrared technique to yield absolute cerebral blood flow measurements. *Biomed Opt Express* 2: 2068-2081, 2011.
30. **Durduran T, Burnett MG, Yu GQ, Zhou C, Furuya D, Yodh AG, Detre JA, and Greenberg JH**. Spatiotemporal quantification of cerebral blood flow during functional activation in rat somatosensory cortex using laser-speckle flowmetry. *J Cerebr Blood F Met* 24: 518-525, 2004.
31. **Durduran T, Choe R, Baker WB, and Yodh AG**. Diffuse Optics for Tissue Monitoring and Tomography. *Rep Prog Phys* 73: 2010.
32. **Durduran T, Zhou C, Buckley EM, Kim MN, Yu G, Choe R, Gaynor JW, Spray TL, Durning SM, Mason SE, Montenegro LM, Nicolson SC, Zimmerman RA, Putt ME, Wang J, Greenberg JH, Detre JA, Yodh AG, and Licht DJ**. Optical measurement of cerebral hemodynamics and oxygen metabolism in neonates with congenital heart defects. *J Biomed Opt* 15: 037004, 2010.
33. **Ferrari M, Binzoni T, and Quaresima V**. Oxidative metabolism in muscle. *Philos Trans R Soc Lond B Biol Sci* 352: 677-683, 1997.
34. **Ferreira LF, Lutjemeier BJ, Townsend DK, and Barstow TJ**. Effects of pedal frequency on estimated muscle microvascular O-2 extraction. *Eur J Appl Physiol* 96: 558-563, 2006.
35. **Ferreira LF, Padilla DJ, Musch TI, and Poole DC**. Temporal profile of rat skeletal muscle capillary haemodynamics during recovery from contractions. *J Physiol* 573: 787-797, 2006.
36. **Ferreira LF, Townsend DK, Lutjemeier BJ, and Barstow TJ**. Muscle capillary blood flow kinetics estimated from pulmonary O2 uptake and near-infrared spectroscopy. *J Appl Physiol (1985)* 98: 1820-1828, 2005.

37. **Grassi B, Pogliaghi S, Rampichini S, Quaresima V, Ferrari M, Marconi C, and Cerretelli P**. Muscle oxygenation and pulmonary gas exchange kinetics during cycling exercise on-transitions in humans. *J Appl Physiol (1985)* 95: 149-158, 2003.
38. **Grassi B, Poole DC, Richardson RS, Knight DR, Erickson BK, and Wagner PD**. Muscle O2 uptake kinetics in humans: implications for metabolic control. *J Appl Physiol (1985)* 80: 988-998, 1996.
39. **Gratton E, Fantini S, Franceschini MA, Gratton G, and Fabiani M**. Measurements of scattering and absorption changes in muscle and brain. *Philos Trans R Soc Lond B Biol Sci* 352: 727-735, 1997.
40. **Gurley K, Shang Y, and Yu G**. Noninvasive optical quantification of absolute blood flow, blood oxygenation, and oxygen consumption rate in exercising skeletal muscle. *J Biomed Opt* 17: 075010, 2012.
41. **Habazettl H, Athanasopoulos D, Kuebler WM, Wagner H, Roussos C, Wagner PD, Ungruhe J, Zakynthinos S, and Vogiatzis I**. Near-infrared spectroscopy and indocyanine green derived blood flow index for noninvasive measurement of muscle perfusion during exercise. *J Appl Physiol (1985)* 108: 962-967, 2010.
42. **Hamaoka T, McCully KK, Quaresima V, Yamamoto K, and Chance B**. Near-infrared spectroscopy/imaging for monitoring muscle oxygenation and oxidative metabolism in healthy and diseased humans. *Journal of Biomedical Optics* 12: 2007.
43. **Heinonen I, Kemppainen J, Kaskinoro K, Peltonen JE, Borra R, Lindroos MM, Oikonen V, Nuutila P, Knuuti J, Hellsten Y, Boushel R, and Kalliokoski KK**. Comparison of exogenous adenosine and voluntary exercise on human skeletal muscle perfusion and perfusion heterogeneity. *J Appl Physiol (1985)* 108: 378-386, 2010.
44. **Heinonen I, Nesterov SV, Kemppainen J, Nuutila P, Knuuti J, Laitio R, Kjaer M, Boushel R, and Kalliokoski KK**. Role of adenosine in regulating the heterogeneity of skeletal muscle blood flow during exercise in humans. *J Appl Physiol (1985)* 103: 2042-2048, 2007.
45. **Hirai T, Visneski MD, Kearns KJ, Zelis R, and Musch TI**. Effects of NO synthase inhibition on the muscular blood flow response to treadmill exercise in rats. *J Appl Physiol (1985)* 77: 1288-1293, 1994.
46. **Jain V, Buckley EM, Licht DJ, Lynch JM, Schwab PJ, Naim MY, Lavin NA, Nicolson SC, Montenegro LM, Yodh AG, and Wehrli FW**. Cerebral oxygen metabolism in neonates with congenital heart disease quantified by MRI and optics. *J Cereb Blood Flow Metab* 34: 380-388, 2014.
47. **Kalliokoski KK, Knuuti J, and Nuutila P**. Blood transit time heterogeneity is associated to oxygen extraction in exercising human skeletal muscle. *Microvasc Res* 67: 125-132, 2004.
48. **Kalliokoski KK, Oikonen V, Takala TO, Sipila H, Knuuti J, and Nuutila P**. Enhanced oxygen extraction and reduced flow heterogeneity in exercising muscle in endurance-trained men. *Am J Physiol Endocrinol Metab* 280: E1015-1021, 2001.
49. **Kindig CA, Richardson TE, and Poole DC**. Skeletal muscle capillary hemodynamics from rest to contractions: implications for oxygen transfer. *J Appl Physiol (1985)* 92: 2513-2520, 2002.
50. **Koga S, Rossiter HB, Heinonen I, Musch TI, and Poole DC**. Dynamic heterogeneity of exercising muscle blood flow and O2 utilization. *Med Sci Sports Exerc* 46: 860-876, 2014.
51. **Laughlin MH, and Armstrong RB**. Muscular blood flow distribution patterns as a function of running speed in rats. *Am J Physiol* 243: H296-306, 1982.
52. **Limberg JK, Eldridge MW, Proctor LT, Sebranek JJ, and Schrage WG**. Alpha-adrenergic control of blood flow during exercise: effect of sex and menstrual phase. *J Appl Physiol (1985)* 109: 1360-1368, 2010.
53. **Lin PY, Roche-Labarbe N, Dehaes M, Carp S, Fenoglio A, Barbieri B, Hagan K, Grant PE, and Franceschini MA**. Non-invasive optical measurement of cerebral metabolism and hemodynamics in infants. *J Vis Exp* e4379, 2013.

54. **Lutjemeier BJ, Ferreira LF, Poole DC, Townsend D, and Barstow TJ**. Muscle microvascular hemoglobin concentration and oxygenation within the contraction-relaxation cycle. *Resp Physiol Neurobi* 160: 131-138, 2008.
55. **Lutjemeier BJ, Miura A, Scheuermann BW, Koga S, Townsend DK, and Barstow TJ**. Muscle contraction-blood flow interactions during upright knee extension exercise in humans. *J Appl Physiol (1985)* 98: 1575-1583, 2005.
56. **Mancini DM, Bolinger L, Li H, Kendrick K, Chance B, and Wilson JR**. Validation of near-infrared spectroscopy in humans. *J Appl Physiol (1985)* 77: 2740-2747, 1994.
57. **McDonough P, Behnke BJ, Kindig CA, and Poole DC**. Rat muscle microvascular PO2 kinetics during the exercise off-transient. *Exp Physiol* 86: 349-356, 2001.
58. **McDonough P, Behnke BJ, Padilla DJ, Musch TI, and Poole DC**. Control of microvascular oxygen pressures in rat muscles comprised of different fibre types. *J Physiol-London* 563: 903-913, 2005.
59. **Moritani T, Tanaka H, Yoshida T, Ishii C, Yoshida T, and Shindo M**. Relationship between Myoelectric Signals and Blood Lactate during Incremental Forearm Exercise. *Am J Phys Med Rehab* 63: 122-132, 1984.
60. **Musch TI, Eklund KE, Hageman KS, and Poole DC**. Altered regional blood flow responses to submaximal exercise in older rats. *J Appl Physiol (1985)* 96: 81-88, 2004.
61. **Musch TI, Haidet GC, Ordway GA, Longhurst JC, and Mitchell JH**. Training effects on regional blood flow response to maximal exercise in foxhounds. *J Appl Physiol (1985)* 62: 1724-1732, 1987.
62. **Okushima D, Poole DC, Barstow TJ, Rossiter HB, Kondo N, Bowen TS, Amano T, and Koga S**. Greater (V)over dotO(2peak) is correlated with greater skeletal muscle deoxygenation amplitude and hemoglobin concentration within individual muscles during ramp-incremental cycle exercise. *Physiological Reports* 4: 2016.
63. **Okushima D, Poole DC, Rossiter HB, Barstow TJ, Kondo N, Ohmae E, and Koga S**. Muscle deoxygenation in the quadriceps during ramp incremental cycling: Deep vs. superficial heterogeneity. *J Appl Physiol (1985)* 119: 1313-1319, 2015.
64. **Piiper J, Pendergast DR, Marconi C, Meyer M, Heisler N, and Cerretelli P**. Blood flow distribution in dog gastrocnemius muscle at rest and during stimulation. *J Appl Physiol (1985)* 58: 2068-2074, 1985.
65. **Poole DC, Wagner PD, and Wilson DF**. Diaphragm microvascular plasma PO2 measured in vivo. *J Appl Physiol (1985)* 79: 2050-2057, 1995.
66. **Ray CA, and Dudley GA**. Muscle use during dynamic knee extension: implication for perfusion and metabolism. *J Appl Physiol* 85: 1194-1197, 1998.
67. **Richardson RS, Poole DC, Knight DR, Kurdak SS, Hogan MC, Grassi B, Johnson EC, Kendrick KF, Erickson BK, and Wagner PD**. High muscle blood flow in man: is maximal O2 extraction compromised? *J Appl Physiol (1985)* 75: 1911-1916, 1993.
68. **Richardson TW, Kindig CA, Musch TI, and Poole DC**. Effects of chronic heart failure on skeletal muscle capillary hemodynamics at rest and during contractions. *J Appl Physiol* 95: 1055-1062, 2003.
69. **Roche-Labarbe N, Carp SA, Surova A, Patel M, Boas DA, Grant RE, and Franceschini MA**. Noninvasive Optical Measures of CBV, StO(2), CBF Index, and rCMRO(2) in Human Premature Neonates' Brains in the First Six Weeks of Life. *Hum Brain Mapp* 31: 341-352, 2010.
70. **Russell JA, Kindig CA, Behnke BJ, Poole DC, and Musch TI**. Effects of aging on capillary geometry and hemodynamics in rat spinotrapezius muscle. *Am J Physiol-Heart C* 285: H251-H258, 2003.
71. **Shang Y, Symons TB, Durduran T, Yodh AG, and Yu GQ**. Effects of muscle fiber motion on diffuse correlation spectroscopy blood flow measurements during exercise. *Biomed Opt Express* 1: 500-511, 2010.
72. **Smith JR, Broxterman RM, Ade CJ, Evans KK, Kurti SP, Hammer SM, Barstow TJ, and Harms CA**. Acute supplementation of N-acetylcysteine does not affect muscle blood flow and oxygenation characteristics during handgrip exercise. *Physiol Rep* 4: 2016.

73. **Smith JR, Hageman KS, Harms CA, Poole DC, and Musch TI**. Respiratory muscle blood flow during exercise: Effects of sex and ovarian cycle. *J Appl Physiol (1985)* 122: 918-924, 2017.
74. **Spencer MD, Murias JM, and Paterson DH**. Characterizing the profile of muscle deoxygenation during ramp incremental exercise in young men. *Eur J Appl Physiol* 112: 3349-3360, 2012.
75. **Van Beekvelt MC, Borghuis MS, van Engelen BG, Wevers RA, and Colier WN**. Adipose tissue thickness affects in vivo quantitative near-IR spectroscopy in human skeletal muscle. *Clin Sci (Lond)* 101: 21-28, 2001.
76. **Vogiatzis I, Habazettl H, Louvaris Z, Andrianopoulos V, Wagner H, Zakynthinos S, and Wagner PD**. A method for assessing heterogeneity of blood flow and metabolism in exercising normal human muscle by near-infrared spectroscopy. *J Appl Physiol (1985)* 118: 783-793, 2015.
77. **Wagner PD**. Diffusive resistance to O2 transport in muscle. *Acta Physiol Scand* 168: 609-614, 2000.
78. **Wagner PD**. Muscle O2 transport and O2 dependent control of metabolism. *Med Sci Sports Exerc* 27: 47-53, 1995.
79. **Yu G, Durduran T, Lech G, Zhou C, Chance B, Mohler ER, 3rd, and Yodh AG**. Time-dependent blood flow and oxygenation in human skeletal muscles measured with noninvasive near-infrared diffuse optical spectroscopies. *J Biomed Opt* 10: 024027, 2005.
80. **Yu GQ, Floyd TF, Durduran T, Zhou C, Wang JJ, Detre JA, and Yodh AG**. Validation of diffuse correlation spectroscopy for muscle blood flow with concurrent arterial spin labeled perfusion MRI. *Opt Express* 15: 1064-1075, 2007.
81. **Zhou C, Eucker SA, Durduran T, Yu GQ, Ralston J, Friess SH, Ichord RN, Margulies SS, and Yodh AG**. Diffuse optical monitoring of hemodynamic changes in piglet brain with closed head injury. *Journal of Biomedical Optics* 14: 2009.